immediately. The mixture was stirred for 5 min. The solid was isolated and dried in vacuo: ^{1}H NMR (CD_2Cl_2) δ 2.51 (br, 3, CH_3CN), 2.2 (s, 15, C_5Me_5), 1.2 (s, 6, WMe); ^{13}C NMR (CD_2Cl_2) δ 117.4 (C_5Me_5), 110.2 (CH_3CN), 33.4 (WCH_3), 11.3 (C_5Me_5), 4.25 (CH_3CN).

X-ray Crystal Structure of $[WCp^*Me_2SMes]_2(\mu\text{-}N_2)$ (2f). Data were collected at −65 °C on an Enraf-Nonius CAD4 diffractometer equipped with a liquid nitrogen low-temperature device and using graphite monochromated Mo Kα radiation (λ = 0.71069 Å). A total of 21 931 reflections were collected, 7188 of which were unique. Equivalent reflections were merged. The intensities of three representative reflections which were measured after every 60 min of X-ray exposure time declined by 28%. A linear correction factor was applied to the data to account for this phenomenon. The structure was solved by direct methods.[23] Refinement was by full-matrix least squares using TEXSAN. Hydrogen atoms were included in calculated positions (d_{C-H} = 0.95 Å). Final R_1 = 0.050 and R_2 = 0.067. Crystal data can be found in Table I.

X-ray Crystal Structure of $[WCp^*Me_2(OC_6F_5)]_2(\mu\text{-}N_2)$ (2d). Data were collected at 23 °C on a Rigaku AFC6 diffractometer with graphite monochromated Mo Kα radiation (λ = 0.71069 Å) and a 12 KW rotating anode generator. A total of 4476 reflections were collected, 4209 of which were unique. Equivalent reflections were merged. The intensities of three representative reflections which were measured after every 150 reflections remained constant throughout data collection indicating crystal and electronic stability. Therefore, no decay correction was applied. The structure was solved by the Patterson method. Refinement was by full-matrix least squares using TEXSAN. Hydrogen atoms were included in calculated positions (d_{C-H} = 0.95 Å). Final R_1 = 0.057 and R_2 = 0.077. Crystal data can be found in Table I.

Acknowledgment. R.R.S. thanks the National Institutes of Health for support through Grant GM 31978. We also thank the U.S. Department of Energy, Division of University and Industry Programs, for funds to purchase the X-ray diffractometer (Grant DE-FG05-86ER 75292) and Dr. W. A. Nugent for a sample of perfluoropinacolate.

Registry No. 1, 96999-48-3; **2a**, 126017-96-7; **2b**, 126017-97-8; **2c**, 126018-01-7; **2d**, 126018-02-8; **2e**, 126018-05-1; **2f**, 126018-04-0; **2g**, 126018-03-9; **3a**, 126017-98-9; **3b**, 126018-00-6; **4a**, 126035-21-0; **4b**, 126018-06-2; $WCp^*Me_3(OTf)$, 126017-94-5; WCp^*Me_4, 96055-89-9; $[WCp^*Me_4]^+PF_6^-$, 96999-45-0; $WCp^*Me_3(NNH_2)$, 96999-47-2; WCp^*Cl_4, 96055-85-5; $WCp^*Me_3(CH_2)$, 108713-51-5; WCp^*Me_5, 108713-47-9; $[WCp^*Me_3]_2(\mu\text{-}^{15}N_2)$, 126017-95-6; $\{[WCp^*Me_2(CH_3CN)]_2(\mu\text{-}N_2)\}^{2+}(BF_4^-)_2$, 126018-08-4; ^{15}N, 14390-96-6.

Supplementary Material Available: A fully labeled drawing and an ORTEP drawing and tables of final positional parameters and anisotropic thermal parameters for $[WCp^*Me_2(OC_6F_5)]_2(\mu\text{-}N_2)$ and $[WCp^*Me_2(SMes)]_2(\mu\text{-}N_2)$ (16 pages); tables of observed and calculated structure factors (72 pages). Ordering information is given on any current masthead page.

Preparation and Characterization of Two High Oxidation State Molybdenum Dinitrogen Complexes: $[MoCp^*Me_3]_2(\mu\text{-}N_2)$ and $[MoCp^*Me_3](\mu\text{-}N_2)[WCp'Me_3]$

Richard R. Schrock,* Richard M. Kolodziej, Andrew H. Liu, William M. Davis, and Michael G. Vale

Contribution from the Department of Chemistry 6-311, Massachusetts Institute of Technology, Cambridge, Massachusetts 02139. *Received August 17, 1989*

Abstract: $[MoCp^*Cl_4]_2$ ($Cp^* = C_5Me_5$) is alkylated by MeMgCl in tetrahydrofuran to give red microcrystalline $MoCp^*Me_4$ in ~70% yield. $MoCp^*Me_4$ reacts with 1 equiv of $HOSO_2CF_3$ in ether to give purple microcrystalline $MoCp^*Me_3(OSO_2CF_3)$ in ~85% yield. Triflate can be displaced readily from $MoCp^*Me_3(OSO_2CF_3)$ by adding LiOR (OR = pentafluorophenoxide, 2,6-diisopropylphenoxide, 2,6-dimethoxyphenoxide, 2,4,6-trimethoxyphenoxide, 2,6-dimethyl-4-methoxyphenoxide, and catecholate) in ether to yield complexes of the type $MoCp^*Me_3(OR)$ ($MoCp^*Me_2(cat)$ in the case of catecholate) in 50–80% yield. Cyclic voltammograms of the $MoCp^*Me_3(OR)$ complexes display quasi-reversible oxidation waves in the region 0.29 to −0.50 V, and the complexes can be oxidized chemically (with the exception of OR = pentafluorophenoxide and catecholate) by $[FeCp_2][PF_6]$ in methylene chloride to give complexes of the type $[MoCp^*Me_3(OR)][PF_6]$ as orange-brown microcrystalline powders in 80–90% yield. Addition of 3 equiv of hydrazine to $[MoCp^*Me_3(OR)][PF_6]$ in ether provides $[MoCp^*Me_3]_2(\mu\text{-}N_2)$ in low yield after purification by filtration through alumina and recrystallization from ether. $[MoCp^*Me_3]_2(\mu\text{-}N_2)$ belongs to the space group $P2_1/n$ with a = 12.895 (5) Å, b = 16.443 (6) Å, c = 14.556 (5) Å, β = 115.87 (3)°, V = 2777 (4) Å^3, Z = 4. Final R = 0.032 and R_w = 0.043. It contains two pseudo-square-pyramidal molybdenum atoms (axial Cp*), one of which is twisted by ~90° with respect to the other. Mo–N–N angles are nearly linear (176.7 (2)° and 172.0 (2)°), Mo–N bonds are fairly short (1.819 (2) Å and 1.821 (3) Å), and N–N is 1.236 (3) Å. $[MoCp^*Me_3](\mu\text{-}N_2)[WCp'Me_3]$ can be prepared by treating $WCp'Me_3(NNH_2)$ ($Cp' = C_5Me_4Et$) with $[MoCp^*Me_3(OR)][PF_6]$ in ether in the presence of NEt_3 and is isolated by recrystallization from ether/pentane; it is contaminated with $[WCp'Me_3]_2(\mu\text{-}N_2)$. $[MoCp^*Me_3](\mu\text{-}N_2)[WCp'Me_3]$ belongs to the space group $P2_1/n$ with a = 13.46 (2) Å, b = 16.46 (2) Å, c = 14.48 (2) Å, β = 116.92 (9)°, V = 2861 (6) Å^3, Z = 4. Final R = 0.031 and R_w = 0.043. The structure is nearly identical with that of $[MoCp^*Me_3]_2(\mu\text{-}N_2)$. It contains pseudo-square-pyramidal molybdenum and tungsten atoms (Cp* and Cp′ axial), one of which is twisted by ~90° with respect to the other. Mo–N(1)–N(2) and W–N(2)–N(1) are nearly linear at 176.6 (4) and 174.1 (4)°, respectively, Mo–N(1) and W–N(2) are 1.816 (5) and 1.816 (7) Å, respectively, and N(1)–N(2) is 1.235 (7) Å. Addition of excess acid to $[MoCp^*Me_3](\mu\text{-}N_2)[WCp'Me_3]$ in the presence of excess zinc amalgam converts 90% of the coordinated dinitrogen ligand into ammonia (1.80 equiv), whereas $[MoCp^*Me_3]_2(\mu\text{-}N_2)$ and $[WCp^*Me_3]_2(\mu\text{-}N_2)$ under similar conditions yield less than half of the of the available nitrogen as ammonia.

In the previous paper[1] we described some W=N—N=W complexes that contain a highly reduced bridging dinitrogen ("hydrazido(4–)") ligand with a relatively long N–N bond (~1.30 Å) and short W–N bonds (~1.75 Å),[2] including $[WCp^*Me_3]_2(\mu\text{-}N_2)$ and derivatives of the type $[WCp^*Me_2X]_2(\mu\text{-}N_2)$ (X = Cl, OSO_2CF_3, thiolate, phenoxide). Since molybdenum-containing nitrogenases are the most common and most active, and since calculations indicate that the Mo–N

(1) O'Regan, M. B.; Liu, A. H.; Finch, W. C.; Schrock, R. R.; Davis, W. M., preceding paper in this issue.

(2) Churchill, M. R.; Li, Y. J. *J. Organomet. Chem.* **1980**, *301*, 49.

0002-7863/90/1512-4338$02.50/0

Table I. EPR Data for the $MoCp^*Me_3X$ Complexes in Dichloromethane[a]

compound	g	$\Delta\nu_{1/2}$[b]	a_{Mo}[b]	a_H[b]
$MoCp^*Me_4$	2.011	28		
$MoCp^*Me_3(OSO_2CF_3)$	2.002	16	37	5
$MoCp^*Me_2(O_2C_6H_4)$	2.003	13	36	5
$MoCp^*Me_3(OC_6F_5)$	2.000	14	39	
$MoCp^*Me_3$(DIPP)	1.997	11	38	
$MoCp^*Me_3$(DMMP)	1.994	14	37	
$MoCp^*Me_3$(DOMP)	1.995	14	38	
$MoCp^*Me_3$(TROMP)	1.995	15	37	

[a] X-band. [b] Gauss.

bonds in $[MCl_4(\mu\text{-}N_2)MCl_4]$ (M = Mo, W) complexes are weaker than analogous W–N bonds,[3] it is important to establish that molybdenum complexes analogous to those described for tungsten can be prepared and to compare and contrast structures and reactivities.

In this paper we discuss the synthesis, X-ray diffraction studies, and generation of ammonia by two high oxidation state molybdenum dinitrogen complexes, $[MoCp^*Me_3]_2(\mu\text{-}N_2)$ and $[MoCp^*Me_3](\mu\text{-}N_2)[WCp'Me_3]$ ($Cp^* = C_5Me_5$; $Cp' = C_5Me_4Et$) as well as the preparation and characterization of a series of $MoCp^*Me_3(OR)$ and $[MoCp^*Me_3(OR)][PF_6]$ complexes (OR = substituted phenoxide) that serve as synthetic precursors to the dinitrogen complexes.

Results

Preparation of $MoCp^*Me_4$ and $MoCp^*Me_3(OSO_2CF_3)$. Alkylation of $[MoCp^*Cl_4]_2$[4] proceeds in good yield if it is added as a solid to a dilute solution of the Grignard reagent in THF (eq 1); addition of Grignard to $[MoCp^*Cl_4]_2$ is not successful, ap-

$$[MoCp^*Cl_4]_2 + 9MeMgCl \xrightarrow[-MgCl_2]{THF} \underset{60\text{–}80\%}{MoCp^*Me_4} \quad (1)$$

parently because the metal is reduced. After the reaction is stirred for 2 h at 25 °C and the solvent is removed in vacuo, $MoCp^*Me_4$ can be extracted from the residue into pentane. Red microcrystalline $MoCp^*Me_4$ is usually pure enough for further use if it is collected as the pentane is removed in vacuo. $MoCp^*Me_4$ also can be recrystallized from either cold pentane or ether, or it may be sublimed in vacuo (60 °C, <0.005 μm). The EPR spectrum of $MoCp^*Me_4$ at 25 °C is that expected for a d^1 ion ($\langle g\rangle = 2.011$, $\Delta\nu_{1/2} = 28$ G).

The cyclic voltammogram of $MoCp^*Me_4$ in methylene chloride displays an irreversible oxidation wave at 0.10 V (vs Ag/Ag^+), and $MoCp^*Me_4$ decomposes when treated with $[FeCp_2][PF_6]$. This behavior contrasts strongly with that observed for the analogous tungsten system where $[WCp^*Me_4][PF_6]$ is an isolable species prepared by chemical oxidation of WCp^*Me_4 by $[FeCp_2][PF_6]$.[1] However, these results are consistent with what one might predict on the basis of the generally greater stability of high oxidation state complexes of tungsten versus molybdenum. Methyl groups in the molybdenum cation also might be considerably more susceptible to intramolecular and/or intermolecular α hydrogen abstraction processes than those in the analogous tungsten complex.

$MoCp^*Me_4$ reacts with 1 equiv of triflic acid in ether to give $MoCp^*Me_3(OSO_2CF_3)$ in good yield (eq 2). $MoCp^*Me_3(OSO_2CF_3)$ precipitates from the reaction mixture as a purple microcrystalline solid that is pure enough for further use. It displays an EPR spectrum at 25 °C ($\langle g\rangle = 2.002$, $\Delta\nu_{1/2} = 16$ G, $a_{Mo} = 37$ G, $a_H = 5$ G). The cyclic voltammogram of $MoCp^*Me_3(OSO_2CF_3)$ in methylene chloride displays an irreversible oxidation wave at 0.63 V and two irreversible reduction waves at −1.09 and −1.67 V (vs Ag/Ag^+; see Table II). Since

$$MoCp^*Me_4 + HOSO_2CF_3 \xrightarrow[-CH_4]{ether} \underset{80\%}{MoCp^*Me_3(OSO_2CF_3)} \quad (2)$$

(3) Rappe, A. K. *Inorg. Chem.* **1986**, *25*, 4686.
(4) Murray, R. C.; Blum, L.; Liu, A. H.; Schrock, R. R. *Organometallics* **1985**, *4*, 954.

Table II. Electrochemical Data for the $MoCp^*Me_3X$ Complexes in Dichloromethane[a]

compound	E_{ox}[b]	E_{red}[b]	$E_{1/2(ox)}$[c]	$E_{1/2(red)}$[c]
$MoCp^*Me_4$	0.10			
$MoCp^*Me_3(OSO_2CF_3)$	0.63	−1.09, −1.67		
$MoCp^*Me_2(O_2C_6H_4)$			0.29	−1.49
$MoCp^*Me_3(OC_6F_5)$		−1.69	0.06	
$MoCp^*Me_3$(DIPP)			−0.34	
$MoCp^*Me_3$(DMMP)			−0.40	
$MoCp^*Me_3$(DOMP)			−0.41	
$MoCp^*Me_3$(TROMP)			−0.50	

[a] All measurements were recorded under N_2 with ~0.1 M $[N(n\text{-}Bu)_4][PF_6]$ as supporting electrolyte. All potentials are referenced to Ag/Ag^+ in CH_3CN; scan range was −2.0 to +2.0 V. [b] Irreversible. [c] Quasi-reversible.

$MoCp^*Me_3(OC_6F_5)$ cannot be chemically oxidized to $[MoCp^*Me_3(OC_6F_5)][PF_6]$ (see below), one would not expect to be able to isolate $[MoCp^*Me_3(OSO_2CF_3)][PF_6]$. The triflate ligand is a poor electron donor, leaving the metal relatively cationic and difficult to oxidize.

Unlike $WCp^*Me_3(OSO_2CF_3)$, which can be reduced with excess Na/Hg in ether under N_2 to yield $[WCp^*Me_3]_2(\mu\text{-}N_2)$ in high yield,[1] $MoCp^*Me_3(OSO_2CF_3)$ decomposes to an uncharacterizable mixture of complexes when treated with Na/Hg, gallium, or zinc under conditions analogous to those used to prepare $[WCp^*Me_3]_2(\mu\text{-}N_2)$.

Preparation of $MoCp^*Me_3(OR)$ and $[MoCp^*Me_3(OR)][PF_6]$. $MoCp^*Me_3(OR)$ (OR = pentafluorophenoxide (OC_6F_5), 2,6-diisopropylphenoxide (DIPP), 2,6-dimethoxyphenoxide (DOMP), 2,6-dimethoxy-4-methylphenoxide (DMMP), or 2,4,6-trimethoxyphenoxide (TROMP)) can be prepared by treating $MoCp^*Me_3(OSO_2CF_3)$ with the desired phenoxide salt in ether (eq 3). A related catecholate complex, $MoCp^*Me_2$(cat), can be

$$MoCp^*Me_3(OSO_2CF_3) + LiOR \xrightarrow[-LiOSO_2CF_3]{ether} \underset{50\text{–}80\%}{MoCp^*Me_3(OR)} \quad (3)$$

prepared by adding 1 equiv of $LiO(HO)C_6H_4$ to $MoCp^*Me_3(OSO_2CF_3)$. Filtration, followed by removal of the solvent in vacuo and then extraction with pentane, effectively separates the $MoCp^*Me_3(OR)$ complexes from $LiOSO_2CF_3$. The red-purple $MoCp^*Me_3(OR)$ complexes can be purified by recrystallization from cold ether as dark blocks or plates.

EPR data for these d^1 species are summarized in Table I and electrochemical data in Table II. EPR signals at 25 °C are observed that have $\langle g\rangle$ values in the range 1.994–2.003 and coupling to ^{97}Mo ($S = 5/2$) and ^{95}Mo ($S = 5/2$) of the order of 38 G. Cyclic voltammograms show electrochemically reversible oxidation waves in the range 0.29 to −0.50 V (+5/+6 couple). Peak separations ($E_{pa} - E_{pc}$) for the oxidations are of the order of 110–200 mV, and $i_{pc}/i_{pa} \approx 0.9\text{–}1.0$ at scan rates of 200 mV s^{-1}. The data in Table II indicate that as more electron-donating phenoxide ligands are used, $MoCp^*Me_3(OR)$ complexes become easier to oxidize, and oxidation products are stable on the electrochemical time scale. If phenol pK_a values are considered, then $MoCp^*Me_3(OC_6F_5)$ should be the most difficult complex to oxidize and $MoCp^*Me_3$(TROMP) the easiest, in agreement with the results obtained.

$[MoCp^*Me_3(OR)][PF_6]$ (OR = DIPP, DOMP, DMMP, and TROMP) can be prepared by chemical oxidation of the $MoCp^*Me_3(OR)$ species with $[FeCp_2][PF_6]$ (eq 4). The cationic

$$MoCp^*Me_3(OR) + [FeCp_2][PF_6] \xrightarrow[-FeCp_2]{CH_2Cl_2} \underset{80\text{–}90\%}{[MoCp^*Me_3(OR)][PF_6]} \quad (4)$$

species are precipitated in 80–90% yield from methylene chloride as microcrystalline powders upon addition of pentane to the reaction mixture. They are exceedingly soluble in chlorinated solvents, moderately soluble in THF, and insoluble in ether or pentane. They are formally 14-electron species not counting

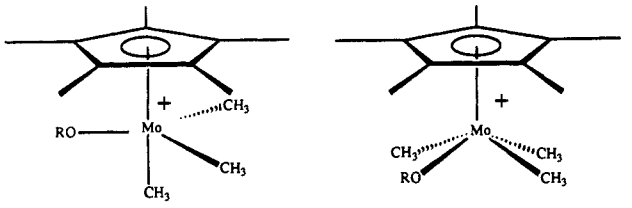

a b

Figure 1. Two most likely geometries for the $[MoCp^*Me_3(OR)][PF_6]$ complexes.

π-bonding from the phenoxide ligands. Chemical oxidation of $MoCp^*Me_3(OC_6F_5)$ by $[FeCp_2][PF_6]$ failed to yield a stable cationic species, while $MoCp^*Me_2(O_2C_6H_4)$ does not react with $[FeCp_2][PF_6]$.

NMR spectra of the $[MoCp^*Me_3(OR)][PF_6]$ species at 25 °C show two types of Mo–CH_3 groups in a 2:1 ratio, suggesting that the geometry is either a square pyramid or a trigonal bipyramid (Figure 1). A square pyramid seems more likely since all but one of the structurally characterized $MCpL_4$ complexes are square pyramidal.[5] (An X-ray study of $W(\eta^5\text{-}C_5Et_3Me_2)Me_4$[6] shows it to be a square pyramid, and so we assume that WCp^*Me_4 is also a square pyramid, but an X-ray study of $[WCp^*Me_4][PF_6]$[7] shows that it is a trigonal bipyramid at low temperature. Electrochemical studies of the $WCp^*Me_4/WCp^*Me_4^+$ couple confirm that the structure of $[WCp^*Me_4][PF_6]$ is not the same as WCp^*Me_4, since the oxidation wave at −0.11 V has a 560 mV $E_{pc} - E_{pa}$ peak separation.[7]) The square-pyramidal geometry for $MoCp^*Me_3(OR)$ should be favored over a trigonal-bipyramidal geometry in which the OR ligand is in an axial position (trans to the Cp* ligand) because π-bonding between the phenoxide and the metal is expected to be stronger in the former. Since the first oxidation wave for each $MoCp^*Me_3(OR)$ complex has an $E_{pc} - E_{pa}$ peak separation of the order of 110–200 mV, little if any structural rearrangement must take place on going from $MoCp^*Me_3(OR)$ to $[MoCp^*Me_3(OR)]^+$. Therefore we believe that the $[Cp^*MoMe_3(OR)][PF_6]$ complexes most likely also are square pyramids.

Preparation of $[MoCp^*Me_3]_2(\mu\text{-}N_2)$ and $[MoCp^*Me_3](\mu\text{-}N_2)[WCp'Me_3]$. $[MoCp^*Me_3]_2(\mu\text{-}N_2)$ is prepared by treating a suspension of $[MoCp^*Me_3(DIPP)][PF_6]$ in cold ether with 3 equiv of hydrazine (eq 5). The cation reacts in 5–10 min to yield a

$$2[MoCp^*Me_3(DIPP)][PF_6] + 3N_2H_4 \xrightarrow[-2[N_2H_5][PF_6],\ -2HDIPP]{\text{ether}} [MoCp^*Me_3]_2(\mu\text{-}N_2)\ (16\%) \quad (5)$$

red solution that contains a light tan precipitate (presumably $[N_2H_5][PF_6]$). Considerable amounts of $MoCp^*Me_3(DIPP)$, HDIPP, and other Cp*-containing side products are formed. Filtration of a solution of the crude product through alumina removes most of the undesired products. Recrystallization from ether yields virtually black crystals of diamagnetic $[MoCp^*Me_3]_2(\mu\text{-}N_2)$ that redissolve to give red solutions.

The presence of significant amounts of $MoCp^*Me_3(DIPP)$ in the reaction mixture suggested that the primary reaction pathway is the undesired reduction of $[MoCp^*Me_3(DIPP)][PF_6]$ by hydrazine. A potential solution to this problem would be to employ $[MoCp^*Me_3(OR)][PF_6]$ species that are more difficult to reduce than $[MoCp^*Me_3(DIPP)][PF_6]$, such as $[MoCp^*Me_3(DOMP)][PF_6]$, $[MoCp^*Me_3(DMMP)][PF_6]$, or $[MoCp^*Me_3(TROMP)][PF_6]$.

When a suspension of $[MoCp^*Me_3(DOMP)][PF_6]$ in ether is treated with 3 equiv of hydrazine, a colorless solution and a white precipitate form immediately. The reaction mixture then begins to turn the red color characteristic of $[MoCp^*Me_3]_2(\mu\text{-}N_2)$. An ^1H NMR spectrum of the crude red solid shows that $[MoCp^*Me_3]_2(\mu\text{-}N_2)$ is present along with varying amounts of what is probably $MoCp^*Me_3(O)$[8] and other Cp*-containing side products. However, no $MoCp^*Me_3(DOMP)$ is found. Unfortunately, we have not yet been able to isolate the nitrogen complex from these reaction mixtures by recrystallization or chromatography. Likewise, we have not been able to isolate the colorless intermediate that is observed in the initial stages of the reaction. We speculate that it is a hydrazine adduct of $[MoCp^*Me_3(DOMP)][PF_6]$ or a hydrazido(1−) species (possibly $MoCp^*Me_3(DOMP)(NHNH_2)$). Such species would be analogous to the more stable tungsten complexes, $[WCp^*Me_4(NH_2NH_2)][PF_6]$ and $WCp^*Me_4(NHNH_2)$.[9]

The mechanism of reactions between hydrazine and the cations is still obscure. In the analogous reaction between $[WCp^*Me_4][PF_6]$ and hydrazine, $[WCp^*Me_4(NH_2NH_2)][PF_6]$ is formed first.[9] Hydrazine then deprotonates $[WCp^*Me_4(NH_2NH_2)][PF_6]$ to give $WCp^*Me_4(NHNH_2)$, from which methane is lost to give $WCp^*Me_3(NNH_2)$. A related set of reactions involving the hydrazido(2−) ligand in $WCp^*Me_3(NNH_2)$ then leads to $[WCp^*Me_3]_2(\mu\text{-}N_2)$.

$[MoCp^*Me_3](\mu\text{-}N_2)[WCp'Me_3]$ (Cp' = C_5Me_4Et) can be prepared by the reaction of $WCp'Me_3(NNH_2)$[9] with $[MoCp^*Me_3(OR)][PF_6]$ in ether in the presence of triethylamine (eq 6). The yield and selectivity of this reaction depends on the

$$WCp'Me_3(NNH_2) + [MoCp^*Me_3(OR)][PF_6] \xrightarrow[-[HNEt_3][PF_6]-HOR]{NEt_3,\ \text{ether}} [WCp'Me_3]_2(\mu\text{-}N_2) + (OR = DOMP\ 5\text{–}10\%,\ DIPP\ 6\text{–}8\%)\ [MoCp^*Me_3](\mu\text{-}N_2)[WCp'Me_3] \quad (6)$$
$$(OR = DOMP\ 40\text{–}45\%,\ DIPP\ 12\text{–}14\%)$$

cation employed. When $[MoCp^*Me_3(DIPP)][PF_6]$ is employed, significant amounts of $MoCp^*Me_3(DIPP)$ again are formed. It is unclear at this stage how $[WCp'Me_3]_2(\mu\text{-}N_2)$ is formed. However, it is known that $[WCp^*Me_3]_2(\mu\text{-}N_2)$ can be prepared from a variety of starting materials under a wide variety of conditions that are at present being explored in more detail.[10] Multiple recrystallizations of the crude residue from the reaction between $WCp'Me_3(NNH_2)$ and $[MoCp^*Me_3(DOMP)][PF_6]$, $[MoCp^*Me_3(DMMP)][PF_6]$, or $[MoCp^*Me_3(TROMP)][PF_6]$ from a mixture of ether and pentane (~3:1) yields large brown cubes of $[MoCp^*Me_3](\mu\text{-}N_2)[WCp'Me_3]$ contaminated by 3–15% $[WCp'Me_3]_2(\mu\text{-}N_2)$. It is not necessary to filter the crude reaction mixture through alumina. The ^1H NMR spectrum of $[MoCp^*Me_3](\mu\text{-}N_2)[Cp'WMe_3]$ at 25 °C displays four types of M–CH_3 resonances in a 2:2:1:1 ratio, consistent with two sets of cis and trans methyl ligands in the equatorial plane of a square pyramid.

The IR spectra of $[MoCp^*Me_3]_2(\mu\text{-}N_2)$ and $[MoCp^*Me_3](\mu\text{-}N_2)[WCp^*Me_3]$ as films (by solvent evaporation) on KBr are similar to those of $[WCp^*Me_3]_2(\mu\text{-}N_2)$.[1] Although ^{15}N-labeling studies have not yet been done, we tentatively assign a peak at 833 cm^{-1} in the spectrum of $[MoCp^*Me_3]_2(\mu\text{-}N_2)$ to the Mo=N stretch[1] and the *two* peaks at 842 and 862 cm^{-1} in the spectrum of $[MoCp^*Me_3](\mu\text{-}N_2)[WCp^*Me_3]$ to ν(Mo=N) and ν(W=N), respectively. These values should be compared with that for ν(W=N) at 889 cm^{-1} in $[WCp^*Me_3]_2(\mu\text{-}N_2)$; 889 cm^{-1} is consistent with the M=N bond being strongest and $\mu\text{-}N_2$ being most reduced in $[WCp^*Me_3]_2(\mu\text{-}N_2)$.

X-ray Studies of $[MoCp^*Me_3]_2(\mu\text{-}N_2)$ and $[MoCp^*Me_3](\mu\text{-}N_2)[WCp'Me_3]$. Table III summarizes the important experimental details concerning the X-ray study of $[MoCp^*Me_3]_2(\mu\text{-}N_2)$, and Table IV lists important bond distances and angles. The final

(5) Kubacek, P.; Hoffmann, R.; Havlas, Z. *Organometallics* **1982**, *1*, 180.
(6) (a) Schrock, R. R.; Pedersen, S. F.; Churchill, M. R.; Ziller, J. W. *Organometallics* **1984**, *3*, 1574. (b) Murray, R. C. Ph.D. Thesis, Massachusetts Institute of Technology, 1985.
(7) Liu, A. H.; Murray, R. C.; Dewan, J. C.; Santarsiero, B. D.; Schrock, R. R. *J. Am. Chem. Soc.* **1987**, *109*, 4282.
(8) $MoCp^*Me_3(O)$ can sometimes be isolated in low yields from this reaction as a yellow solid: ^1H NMR (C_6D_6) δ 1.39 (s, 15, $C_5(CH_3)_5$), 1.55 (s, 6, $Mo(CH_3)_{cis}$), 0.44 (s, 3, $Mo(CH_3)_{trans}$).
(9) Schrock, R. R.; Liu, A. H.; O'Regan, M. B.; Finch, W. C.; Payack, J. F. *Inorg. Chem.* **1988**, *27*, 3574.
(10) Glassman, T. G.; Schrock, R. R. To be published.

Table III. X-ray Data for $[MoCp^*Me_3]_2(\mu\text{-}N_2)$ and $[MoCp^*Me_3](\mu\text{-}N_2)[WCp'Me_3]$

	$[MoCp^*Me_3]_2(\mu\text{-}N_2)$	$[MoCp^*Me_3](\mu\text{-}N_2)[WCp'Me_3]$
Crystal Parameters		
crystal system	monoclinic	monoclinic
space group	$P2_1/n$	$P2_1/n$
a	12.895 (5) Å	13.46 (2) Å
b	16.443 (6) Å	16.46 (2) Å
c	14.556 (5) Å	14.48 (2) Å
β	115.87 (3)°	116.92 (9)°
V	2777 (4) Å^3	2861 (6) Å^3
Z	4	4
ρ(calcd)	1.388 g cm^{-3}	1.609 g cm^{-3}
temperature	−65 °C	−65 °C
μ	8.96 cm^{-1}	49.88 cm^{-1}
Intensity Measurement Data		
diffractometer	Enraf-Nonius CAD-4	Rigaku AFC6R
radiation	Mo Kα (λ = 0.71069 Å)	Mo Kα (λ = 0.71069 Å)
monochromator	graphite crystal	graphite crystal
scan type	ω	ω–2θ
scan speed	1.1–10.0°/min	32°/min
scan range	$3° < 2\theta < 55°$	$4° < 2\theta < 55°$
reflcns measd	$+h,+k,\pm l$	$+h,+k,\pm l$
reflcns collected	6581 unique; 5489 $I_o > 3\sigma(I_o)$	6804 unique; 4810 $I_o > 3\sigma(I_o)$
R	0.032	0.031
R_w	0.043	0.045

Table IV. Selected Bond Distances (Å) and Angles (deg) in $[MoCp^*Me_3]_2(\mu\text{-}N_2)$[a]

Mo(2)–N(2)–N(1)	172.0 (2)	C(27)–Mo(2)–C(28)	74.5 (2)
Mo(1)–N(1)–N(2)	176.7 (2)	C(26)–Mo(2)–C(28)	135.4 (2)
N(1)–Mo(1)–C(17)	86.5 (1)	N(1)–N(2)	1.236 (3)
N(1)–Mo(1)–C(16)	85.0 (1)	Mo(1)–N(1)	1.819 (2)
N(1)–Mo(1)–C(18)	121.4 (1)	Mo(2)–N(2)	1.821 (3)
C(17)–Mo(1)–C(18)	74.2 (2)	Mo(1)–C(16)	2.209 (4)
C(16)–Mo(1)–C(18)	74.3 (2)	Mo(1)–C(17)	2.201 (4)
C(16)–Mo(1)–C(17)	136.5 (2)	Mo(1)–C(18)	2.212 (4)
N(2)–Mo(2)–C(26)	86.0 (1)	Mo(2)—C(26)	2.190 (4)
N(2)–Mo(2)–C(28)	85.8 (1)	Mo(2)–C(27)	2.213 (4)
N(2)–Mo(2)–C(27)	125.6 (1)	Mo(2)–C(28)	2.203 (4)
C(26)–Mo(2)–C(27)	75.3 (2)		

[a] Atoms are labeled as shown in Figure 2.

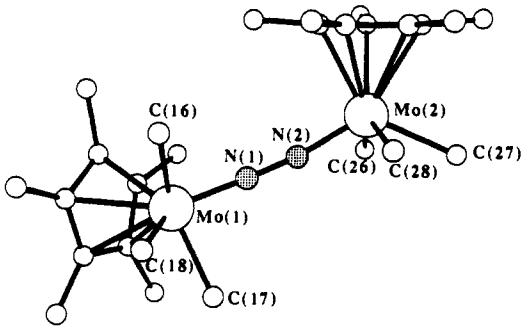

Figure 2. A view of the structure of $[MoCp^*Me_3]_2(\mu\text{-}N_2)$ (hydrogen atoms omitted).

positional parameters can be found in the Supplementary Material.

Figure 2 shows a view of $[MoCp^*Me_3]_2(\mu\text{-}N_2)$. It contains two pseudo-square-pyramidal molybdenum atoms with the Cp* ligands in the axial positions and the three methyl ligands and the nitrogen atom occupying the equatorial positions. The N(1)–Mo(1)–C(16) and N(1)–Mo(1)–C(17) angles (methyls cis to nitrogen) are 85.0 (1) and 86.5 (1)°, respectively (those for Mo(2) are nearly identical), whereas N(1)–Mo(1)–C(18) and N(2)–Mo(2)–C(27) (methyls trans to nitrogen) are 121.4 (1) and 125.6 (1)°, respectively. The C(16)–Mo(1)–C(18) and C(17)–Mo(1)–C(18) angles (cis methyls) are 74.3 (2) and 74.2 (2)° (those for Mo(2) are nearly identical), while C(16)–Mo(1)–C(17) and C(26)–Mo(2)–C(28) (trans methyls) are 136.5 (2) and 135.4 (2)°, respectively.

Table V. Selected Bond Distances (Å) and Angles (deg) in $[MoCp^*Me_3](\mu\text{-}N_2)[WCp'Me_3]$[a]

W–N(2)–N(1)	174.1 (4)	C(5)–W–C(6)	74.7 (3)
Mo–N(1)–N(2)	176.6 (4)	C(4)–W–C(6)	136.2 (3)
N(1)–Mo–C(1)	83.7 (3)	N(1)–N(2)	1.235 (7)
N(1)–Mo–C(3)	87.3 (3)	Mo–N(1)	1.816 (7)
N(1)–Mo–C(2)	118.8 (3)	W–N(2)	1.816 (5)
C(1)–Mo–C(2)	72.9 (3)	Mo–C(1)	2.218 (8)
C(2)–Mo–C(3)	73.2 (3)	Mo–C(2)	2.242 (8)
C(1)–Mo–C(3)	134.9 (3)	Mo–C(3)	2.207 (8)
N(2)–W–C(4)	86.8 (3)	W–C(4)	2.193 (7)
N(2)–W–C(6)	86.3 (3)	W–C(5)	2.230 (7)
N(2)–W–C(5)	125.3 (2)	W–C(6)	2.203 (7)
C(4)–W–C(5)	74.5 (4)		

[a] Atoms are labeled as shown in Figure 3.

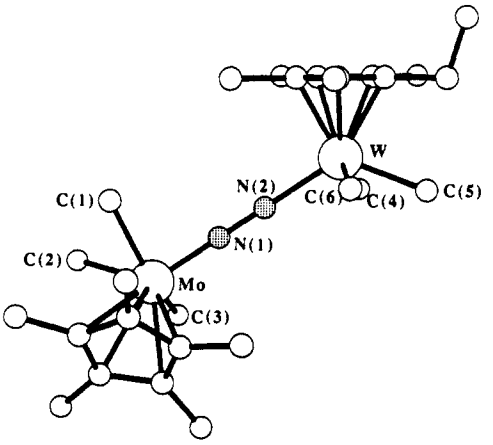

Figure 3. A view of the structure of $[MoCp^*Me_3](\mu\text{-}N_2)[WCp'Me_3]$ (hydrogen atoms omitted).

The molybdenum atoms are connected by an essentially linear N_2 bridge with Mo(1)–N(1)–N(2) and Mo(2)–N(2)–N(1) angles of 176.7 (2) and 172.0 (2)°, respectively. One end of the molecule is rotated with respect to the other resulting in a dihedral angle of ~90° between the planes of the Cp* ligands. The Mo(1)–N(1) and Mo(2)–N(2) bond distances are relatively short (1.819 (2) and 1.821 (3) Å, respectively), characteristic of an "imido-like" multiple molybdenum–nitrogen bond.[11] The N(1)–N(2) distance is 1.236 (3) Å, long compared to the N–N distance in unbound nitrogen (1.0976 Å) and the N–N bond distances in the Chatt-type dinitrogen complexes[12] and consistent with a partially reduced form of dinitrogen. The molybdenum–carbon (methyl) and molybdenum–carbon (Cp*) distances (not listed) are normal, in the range 2.190–2.212 and 2.324–2.436 Å, respectively.

Table III contains a summary of the important experimental details from the X-ray study of $[MoCp^*Me_3](\mu\text{-}N_2)[WCp'Me_3]$. Selected bond distances and angles are listed in Table V. Final positional parameters can be found in the Supplementary Material. Figure 3 shows a view of the molecule. The crystal chosen for the study contained 12% $[WCp'Me_3]_2(\mu\text{-}N_2)$, as determined by systematic variation of occupancy until the thermal parameters of both the tungsten (from $[MoCp^*Me_3](\mu\text{-}N_2)[WCp'Me_3]$) and the tungsten (from the dopant) were equivalent. Apparently $[WCp'Me_3]_2(\mu\text{-}N_2)$ adopts the geometry found for $[MoCp^*Me_3](\mu\text{-}N_2)[WCp'Me_3]$ and $[MoCp^*Me_3]_2(\mu\text{-}N_2)$ not that for $[WCp^*Me_3]_2(\mu\text{-}N_2)$.

The molecular structure of $[MoCp^*Me_3](\mu\text{-}N_2)[WCp'Me_3]$ is essentially identical with that of $[MoCp^*Me_3]_2(\mu\text{-}N_2)$. It contains pseudo-square-pyramidal molybdenum and tungsten atoms, both having axial cyclopentadienyl ligands, three methyl ligands, and a nitrogen atom in the equatorial positions and bent away from the Cp ligands. The N(1)–Mo–C(1) and N(1)–Mo–C(3) angles are 83.7 (3) and 87.3 (3)°, while N(2)–W–C(4) and N(2)–W–C(6) angles are 86.8 (3) and 86.3 (3)°, respectively.

Table VI. Protonation Studies of $[MoCp^*Me_3]_2(\mu\text{-}N_2)$, $[MoCp^*Me_3](\mu\text{-}N_2)[WCp'Me_3]$, and $[W^*CpMe_3]_2(\mu\text{-}N_2)$[a]

complex	acid[b]	solvent	reducing agent[c]	eq NH_3 (no. expts)
Mo/Mo	HCl	THF	none	0.32
Mo/Mo	lut·HCl	THF	Zn/Hg	0.62–0.72 (3)[d]
W/Mo	HCl	THF	none	0.32
W/Mo	lut·HCl	THF	Zn/Hg	1.66–1.86 (6)[d,e]
W/Mo	lut·$HOSO_2CF_3$	THF	Zn/Hg	0.60
W/W	HCl	THF	none	0.34
W/W	lut·HCl	THF	Zn/Hg	0.80–0.88 (4)[d]
W/W	lut·$HOSO_2CF_3$	THF	Zn/Hg	1.20
W/W	lut·$HOSO_2CF_3$	ether	Zn/Hg	0.56
W/W	lut·$HOSO_2CF_3$	ether	Na/Hg	0.76

[a] The yield of hydrazine was <3% in the several cases that were examined. Analysis of a hydrazine sample (Lut·HCl;THF;Zn/Hg) showed that a maximum of 5% ammonia was produced. [b] HCl (25 equiv) was used; 16 equiv of lutidine·HCl or lutidine·$HOSO_2CF_3$. [c] Reducing agent (12 equiv) was used. [d] At least one experiment was performed under argon. No significant decrease in ammonia yield was observed. [e] Ammonia (1.70 equiv) was found in a reaction in which the base distillation step was omitted.

The N(1)–Mo–C(2) and N(2)–W–C(5) angles are 118.8 (3) and 125.3 (2)°, respectively. The C(2)–Mo–C(3) and C(1)–Mo–C(2) angles are 73.2 (3) and 72.9 (3)°, while for tungsten they are 74.5 (4)° (C(4)–W–C(5)) and 74.7 (3)° (C(5)–W–C(6)). C(1)–Mo–C(3) and C(4)–W–C(6) are 134.9 (3) and 136.2 (3)°, respectively.

The molybdenum and tungsten atoms are connected by a nearly linear N–N bridge with Mo–N(1)–N(2) and W–N(2)–N(1) angles of 176.6 (4) and 174.1 (4)°, respectively. As in the case of $[MoCp^*Me_3]_2(\mu\text{-}N_2)$, one end of the molecule is rotated with respect to the other so that the dihedral angles between the planes of the Cp ligands is ~90°. The Mo–N(1) and W–N(2) bond distances are fairly short and virtually identical (1.816 (7) and 1.816 (5) Å, respectively). The N(1)–N(2) distance is 1.235 (7) Å, nearly identical with that in $[MoCp^*Me_3]_2(\mu\text{-}N_2)$. The metal–carbon (methyl) and metal–carbon (cyclopentadienyl) distances (not listed) are all normal, in the range 2.193–2.242 and 2.315–2.448 Å, respectively.

Protonation Studies of the Nitrogen Compounds. $[WCp^*Me_3]_2(\mu\text{-}N_2)$ and either 2 equiv of HCl or $HOSO_2CF_3$ react to give $[WCp^*Me_2(X)]_2(\mu\text{-}N_2)$ (X = Cl, OSO_2CF_3) in good yield (eq 7).[1] In contrast, the reaction of $[MoCp^*Me_3](\mu\text{-}N_2)[WCp'Me_3]$ and $[MoCp^*Me_3]_2(\mu\text{-}N_2)$ with strong protic acids has not yet yielded any isolable compounds. Proton NMR studies of crude reaction mixtures from protonation reactions of the molybdenum dinitrogen complexes indicate that mostly paramagnetic products are formed, suggesting that reduction of the metal is a major complication. The fact that molybdenum is generally easier to reduce than tungsten may help explain why $[MoCp^*Me_3](\mu\text{-}N_2)[Cp'WMe_3]$ and $[MoCp^*Me_3]_2(\mu\text{-}N_2)$ are unstable under conditions where $[WCp^*Me_3]_2(\mu\text{-}N_2)$ is cleanly substituted.

$$[Cp^*WMe_3]_2(\mu\text{-}N_2) + 2HX \xrightarrow[-CH_4]{\text{ether}} [Cp^*WMe_2X]_2(\mu\text{-}N_2) \quad (7)$$
(X = Cl, OSO_2CF_3) 80–90%

When the molybdenum dinitrogen complexes are protonated with excess acid (typically HCl) in THF and the solution is allowed to stir at 25 °C for 24 h, ~15% ammonia (0.30 equiv), in addition to traces of hydrazine, is produced relative to the total amount possible (see Experimental Section for details of the method of quantification). Similar results are found for $[WCp^*Me_3]_2(\mu\text{-}N_2)$ (see Table VI). If the $\mu\text{-}N_2$ ligand is considered a hydrazido(4–) species, then two electrons would be needed (in addition to 6 equiv of H^+) for each N_2^{4-} in order to yield 2 equiv of ammonia. Since there are no obvious electron sources in this system, an electron source was added in the form of zinc amalgam or (in one case) sodium amalgam. The amount of ammonia produced under these conditions is approximately double. Using an excess of lutidine·HCl as a mild source of protons and adding it simultaneously to the molybdenum dinitrogen complexes along with an excess of Zn/Hg as a reducing agent in cold THF yields the most ammonia (eq 8), as much as 1.86 equiv from $[MoCp^*Me_3](\mu\text{-}N_2)[WCp'Me_3]$ and 0.72 equiv from $[MoCp^*Me_3]_2(\mu\text{-}N_2)$. Only traces of hydrazine are found.

$$[MoCp^*Me_3](\mu\text{-}N_2)[WCp'Me_3] \xrightarrow[\text{THF, 24 h}]{\text{excess Zn/Hg and lutidine·HCl}} \underset{\text{(trace of } N_2H_4)}{NH_3\ (\sim 90\%)} \quad (8)$$

$[WCp^*Me_3]_2(\mu\text{-}N_2)$ also can be protonated to yield ammonia in the presence of an electron source. The highest yields (60%) are found when lutidine·$HOSO_2CF_3$ is substituted for lutidine·HCl as the proton source, although the W/Mo complex under these conditions gives less ammonia than when Lut-HCl is employed.

Several of the most successful hydrolysis experiments were repeated under argon instead of dinitrogen, but no significant differences were observed. In the most successful hydrolysis experiment (W/Mo) we analyzed the crude reaction mixture for ammonia directly, i.e., without the base distillation step (see Experimental Section), and again virtually the same result was obtained. We also determined that hydrazine itself did not yield a significant amount of ammonia when carried through the analytical procedure. These data taken together suggest that ammonia is produced at the first stage directly from bound dinitrogen only. There is no evidence that gaseous nitrogen is reduced or that hydrazine is a (free) intermediate.

Discussion

The structures reported here should be compared with others that contain reduced dinitrogen, especially $[WCp^*Me_3]_2(\mu\text{-}N_2)$.[2] The important features of $[WCp^*Me_3]_2(\mu\text{-}N_2)$ are the trans arrangement of the Cp* ligands, the short W–N bond distances (1.742 (17) and 1.763 (18) Å), and the long N–N bond distance (1.334 (26) Å). It is not obvious why $[WCp^*Me_3]_2(\mu\text{-}N_2)$ should have transoid Cp* ligands, whereas $[MoCp^*Me_3]_2(\mu\text{-}N_2)$, $[MoCp^*Me_3](\mu\text{-}N_2)[WCp'Me_3]$, and apparently $[WCp'Me_3]_2(\mu\text{-}N_2)$ (the impurity in $[MoCp^*Me_3](\mu\text{-}N_2)[WCp'Me_3]$) should have cisoid cyclopentadienyl ligands. Crystal packing forces probably are sufficient to stabilize different rotamers. The W–N distances in $[WCp^*Me_3]_2(\mu\text{-}N_2)$ are relatively short and similar to W–N bond distances reported in the literature for tungsten imido complexes (W≡N—R).[11] The N–N bond distance in $[WCp^*Me_3]_2(\mu\text{-}N_2)$ is the longest N–N distance to be reported for a $\mu\text{-}N_2$ species of an early transition-metal complex, consistent with it containing a hydrazido(4–) (N_2^{4-}) ligand instead of a dinitrogen ligand. Statistically, however, the N–N distance in $[WCp^*Me_3]_2(\mu\text{-}N_2)$ is indistinguishable from those reported for $[TaCl_3(PBz_3)(THF)]_2(\mu\text{-}N_2)$ (1.282 (6) Å),[13] $[W(C_6H_5C{\equiv}CC_6H_5)(CH_3OCH_2CH_2OCH_3)Cl_2]_2(\mu\text{-}N_2)$ (1.292 (16) Å),[14] $[Ta(CHCMe_3)(CH_2CMe_3)(PMe_3)_2]_2(\mu\text{-}N_2)$ (1.298 (12) Å),[15] $[Ta(DIPP)_3(THF)]_2(\mu\text{-}N_2)$ (1.32 (1) Å),[16] and $[Ta(S\text{-}2,4,6\text{-}C_6H_2\text{-}i\text{-}Pr_3)_3(THF)]_2(\mu\text{-}N_2)$ (1.29 (6) Å).[16] Longer N–N bond distances (1.35 Å) have been reported in some nickel–dinitrogen–lithium clusters.[17]

(11) (a) Nugent, W. A.; Haymore, B. L. *Coord. Chem. Rev.* **1980**, *31*, 123. (b) Nugent, W. A.; Mayer, J. M. *Metal–Ligand Multiple Bonds*; Wiley and Sons: New York, 1988.

(12) (a) Chatt, J.; Dilworth, J. R.; Richards, R. L. *Chem. Rev.* **1978**, *78*, 589 and references therein. (b) Henderson, R. A.; Leigh, J.; Pickett, C. J. *Adv. Inorg. Radiochem.* **1983**, *27*, 197. (c) *New Trends in the Chemistry of Nitrogen Fixation*; Chatt, J., da Camara Pina, L. M., Richards, P. L., Eds.; Academic Press: New York, 1980. (d) Leigh, G. J. *Trans. Met. Chem.* **1986**, *11*, 118.

(13) (a) Rocklage, S. M.; Schrock, R. R. *J. Am. Chem. Soc.* **1982**, *104*, 3077. (b) Churchill, M. R.; Wasserman, H. J. *Inorg. Chem.* **1982**, *21*, 218.

(14) Churchill, M. R.; Li, Y. J.; Theopold, K. H.; Schrock, R. R. *Inorg. Chem.* **1984**, *23*, 4472.

(15) (a) Turner, H. J.; Fellman, J. D.; Rocklage, S. M.; Schrock, R. R.; Churchill, M. R.; Wasserman, H. J. *J. Am. Chem. Soc.* **1980**, *102*, 7809. (b) Churchill, M. R.; Wasserman, H. J. *Inorg. Chem.* **1981**, *20*, 2899.

(16) Schrock, R. R.; Wesolek, M.; Liu, A. H.; Wallace, K. C.; Dewan, J. C. *Inorg. Chem.* **1988**, *27*, 2050.

(17) (a) Jonas, K. *Angew. Chem., Int. Ed. Engl.* **1973**, *12*, 997. (b) Kruger, C.; Tsay, Y. H. *Angew. Chem., Int. Ed. Engl.* **1973**, *12*, 988. (c) Jonas, K.; Brauer, D. J.; Kruger, C.; Roberts, P. J.; Tsay, Y. H. *J. Am. Chem. Soc.* **1976**, *98*, 74.

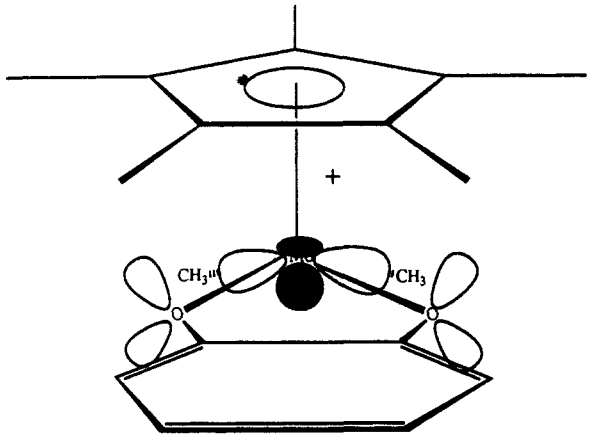

Figure 4. Drawing of $[MoCp^*Me_2(O_2C_6H_4)]^+$ showing poor overlap between the metal LUMO (here d_{xy} orbital) and the p orbitals on the oxygen atoms of the catecholate ligand.

The N–N bond distances for $[MoCp^*Me_3]_2(\mu\text{-}N_2)$ (1.236 (3) Å) and $[MoCp^*Me_3](\mu\text{-}N_2)[WCp'Me_3]$ (1.235 (7) Å) are about a tenth of an angstrom shorter than the N–N distance in $[WCp^*Me_3]_2(\mu\text{-}N_2)$.[2] This difference is small but statistically significant, in spite of the low accuracy of the structure of $[WCp^*Me_3]_2(\mu\text{-}N_2)$, indicating that two tungsten centers are slightly better at reducing the dinitrogen ligand than two molybdenum centers or one molybdenum and one tungsten. This trend is also apparent in the metal–nitrogen bond distances which are about a tenth of an angstrom longer in the molybdenum complexes (Mo–N = 1.819 (2) Å and 1.821 (3) Å in $[MoCp^*Me_3]_2(\mu\text{-}N_2)$; Mo–N = 1.816 (7) Å and W–N = 1.816 (5) in $[MoCp^*Me_3](\mu\text{-}N_2)[WCp'Me_3]$) than in $[WCp^*Me_3]_2(\mu\text{-}N_2)$. The tungsten/molybdenum combination is virtually identical with the molybdenum combination by this criterion. If the $[WCp'Me_3]_2(\mu\text{-}N_2)$ dopant were to influence the structure of $[MoCp^*Me_3](\mu\text{-}N_2)[WCp'Me_3]$, the M–N bond distances would be expected to be shorter and the N–N distance longer in $[MoCp^*Me_3](\mu\text{-}N_2)[WCp'Me_3]$, more like the W–N and N–N distances in $[WCp^*Me_3]_2(\mu\text{-}N_2)$ not those in $[MoCp^*Me_3]_2(\mu\text{-}N_2)$.

π-Bonding in μ-dinitrogen complexes of the type discussed here has been discussed in the preceding paper.[1] π-Bonding from oxygen to molybdenum also must play an important role in stabilizing the Mo(VI) cationic precursors to Mo dinitrogen complexes. The LUMO in complexes of this nature probably is essentially a metal-based ($\sim d_{xy}$) orbital that lies parallel to the C_5 ring (Figure 4). π-Electron density can be donated from an oxygen atom in a typical monodentate alkoxide (phenoxide) ligand, either from an sp^3 or a pure p orbital. The observation that $MoCp^*Me_2(O_2C_6H_4)$ cannot be easily oxidized chemically or electrochemically (see Table II) is consistent with this point of view. As Figure 4 shows, the oxygen p-orbitals are not properly oriented in $MoCp^*Me_2(O_2C_6H_4)$ for overlap with the d_{xy} orbital, and they cannot be rehybridized or the alkoxide rotated as in the case of monoalkoxides. Therefore the cationic charge cannot be stabilized by π donation. A corollary of this analysis is that two or more alkoxides would not be able to stabilize the cation significantly more than one, since only one orbital is readily available to accept π electron density. (What is essentially a d_{z^2} orbital also can accept π electron density, although it also is involved in bonding to the cyclopentadienyl ligand and would not overlap as well with the donor orbital on oxygen.) Preliminary studies suggest that two alkoxides, in fact, are not significantly more stabilizing than one.[18]

Why does the heteronuclear dinitrogen complex, $[MoCp^*Me_3](\mu\text{-}N_2)[WCp'Me_3]$, give nearly 100% conversion of bound N_2 to ammonia when protonated under reducing conditions, while the homonuclear (W or Mo) dinitrogen complexes give only half that under identical conditions? That question is difficult to answer in the absence of knowledge of the details of the mechanism (or mechanisms) of formation of ammonia. It is tempting to speculate that the heterobimetallic nature of the complex is inherently more likely to lead to a splitting of dinitrogen. As discussed previously, paramagnetic molybdenum species were observed when $[MoCp^*Me_3]_2(\mu\text{-}N_2)$ was treated with 2 equiv of acid, and species of the type $[WCp^*Me_2X]_2(\mu\text{-}N_2)$ (X = Cl, OSO_2CF_3) were isolated when $[WCp^*Me_3]_2(\mu\text{-}N_2)$ was treated with 2 equiv of either HCl or $HOSO_2CF_3$. In the case of $[MoCp^*Me_3](\mu\text{-}N_2)[Cp'WMe_3]$, high yields of ammonia could result from mixed-valence species (i.e., Mo(V)/W(VI)) or some other intermediates that have a large dipole moment between the two ends of the nitrogen molecule. A large dipole could facilitate the protonation/electron-transfer steps necessary to reduce the N_2^{4-} ligand to ammonia.

Strong evidence *against* the proposal that two metals are necessary for reduction of dinitrogen are preliminary studies[18] that reveal that $WCp^*Me_3(NNH_2)$ produces close to 2 equiv of ammonia when treated with lutidine·HCl and zinc amalgam in THF. Therefore the yield of ammonia might correlate with the ease of forming $WCp^*Me_3(NNH_2)$. $WCp^*Me_3(NNH_2)$ is not formed from $[WCp^*Me_3]_2(\mu\text{-}N_2)$ readily, as we noted; $[WCp^*Me_3]_2(\mu\text{-}N_2)$ undergoes substitution chemistry with acids. The chemistry of $[MoCp^*Me_3]_2(\mu\text{-}N_2)$ is certainly different from that of $[WCp^*Me_3]_2(\mu\text{-}N_2)$, and most importantly $MoCp^*Me_3(NNH_2)$ has not yet been observed.[18] On the other hand, the Mo≡N bond in the W/Mo species might be cleaved relatively easily to give $WCp^*Me_3(NNH_2)$, and that may be the relatively simple reason why the W/Mo complex yields so much ammonia. The conclusion that one metal may be sufficient for ammonia production is one that has been reached also by researchers studying Chatt-type complexes.[12]

The fact that high oxidation state dinitrogen complexes can produce relatively high yields of ammonia, combined with the fact that $[WCp^*Me_3]_2(\mu\text{-}N_2)$ can be prepared by reducing $WCp^*Me_3(OSO_2CF_3)$, together suggest that coupling the two processes in order to generate ammonia catalytically (with respect to metal) is not out of the question. However, the findings reported here could be taken as evidence that μ-hydrazido(4–) complexes are not part of the most direct pathway to ammonia. Therefore future studies will be aimed at determining how in detail ammonia is produced from hydrazido(2–) species and how hydrazido(2–) species can be prepared directly from dinitrogen.

Experimental Section

General Procedures.[19] $[WCp'Me_4][PF_6]$ and $WCp'Me_3(NNH_2)$ were prepared by using procedures identical with those used to prepare the analogous Cp* derivatives.[1,6,9] $[Cp^*MoCl_4]_2$[4] was prepared by the literature method. Cyclic voltammograms were obtained in a drybox in either methylene chloride or acetonitrile (distilled twice from CaH_2) containing ~0.1 M $[n\text{-}Bu_4N][PF_6]$ as supporting electrolyte. $E_{1/2}$ values are referenced to Ag/Ag^+ and uncorrected for junction potentials. Ammonia and hydrazine were quantified by the indophenol[20] and PDMAB[21] tests, respectively.

Electrochemical data was obtained by using a Princeton Applied Research Model 173 Potentiostat/Galvanostat and Model 175 Universal Programmer, in conjunction with a Houston Instruments RE-0089 X-Y Recorder. Cyclic voltammograms were obtained in the drybox at approximately 25 °C in either dichloromethane (distilled twice from calcium hydride) containing ~0.1 M $[N(n\text{-}Bu)_4][PF_6]$ as supporting electrolyte. $E_{1/2}$ values are referenced to Ag/Ag^+ and uncorrected for junction potentials.

Routine coupling constants are not reported as part of the carbon NMR data.

Preparation of Compounds. $MoCp^*Me_4$. A 3.0 M tetrahydrofuran solution of MeMgCl (119 mmol, 40 mL) was diluted to 250 mL with cold (−35 °C) tetrahydrofuran. This solution was stirred, while $[MoCp^*Cl_4]_2$ (13.4 mmol, 10.0 g) was added slowly as a solid. The temperature was kept below 25 °C. The reaction immediately turns a deep red. After ~2 h of stirring at 25 °C, the reaction mixture was transferred to a flask containing 500 mL of pentane in order to precip-

(18) Vale, M. G. Unpublished results.

(19) Okuda, J.; Murray, R. C.; Dewan, J. C.; Schrock, R. R. *Organometallics* **1986**, *5*, 1681.

(20) Chaney, A. L.; Marbach, E. P. *Clinical Chem.* **1962**, *8*, 130.

(21) Watt, G. W.; Chrisp, J. D. *Anal. Chem.* **1952**, *24*, 2006.

itate the magnesium salts. The salts were removed by filtration through Celite, and the solvent was then removed from the filtrate, leaving a red solid. Extraction of this red solid with ~1 L of pentane (in order to remove any remaining magnesium salts) followed by filtration and concentration of the pentane from the filtrate afforded $MoCp^*Me_4$ in three crops as red microcrystals (5.4 g, 70%), that were pure enough for further use. $MoCpMe_4$ can be further purified by sublimation (60 °C, <0.005 μm) or recrystallization at −35 °C from a minimum volume of either pentane or ether: EPR ⟨g⟩ = 2.011, $\Delta\nu_{1/2}$ = 28 G. Anal. Calcd. for $C_{14}H_{27}Mo$: C. 57.71; H, 9.36; Cl, 0. Found: C, 57.73; H, 9.16; Cl, <0.4.

$MoCp^*Me_3(OSO_2CF_3)$. Triflic acid (18.7 mmol, 1.656 mL) dissolved in 20 mL of cold (−35 °C) ether rapidly and with vigorous stirring to a solution of $MoCp^*Me_4$ (18.7 mmol, 5.451 g) dissolved in 150 mL of cold (−35 °C) ether. The reaction immediately became purple, a purple precipitate formed, and CH_4 evolved. The reaction was allowed to stir for *no more than 30 min*. The purple solid was isolated by filtration, washed with cold ether, and dried in vacuo. Concentration of the filtrate yields another crop of purple $MoCp^*Me_3(OSO_2CF_3)$ (7.1 g, 89%): EPR ⟨g⟩ = 2.002, $\Delta\nu_{1/2}$ = 16 G, coupling to ^{97}Mo (S = 5/2) and ^{95}Mo (S = 5/2) = 37 G, coupling to 6 equiv protons (S = 1/2) = 5 G. Anal. Calcd for $C_{14}H_{24}O_3F_3SMo$: C, 39.53; H, 5.70. Found: C, 39.54; H, 5.64.

$MoCp^*Me_3(DIPP)$. Lithium 2,6-diisopropylphenoxide monoetherate (16.6 mmol, 4.3 g) was added rapidly (as a solid) to a stirred suspension of $MoCp^*Me_3(OSO_2CF_3)$ (16.6 mmol, 7.1 g) in 130 mL of cold (−35 °C) ether. A rapid reaction produced a red solution. Stirring was continued for 2 h, the reaction mixture was then filtered through Celite, and the solvent was removed from the filtrate in vacuo to yield a dark red-purple semicrystalline solid. This purple solid was extracted with ~1 L of pentane. The mixture was then filtered through Celite, and the solvent was removed from the filt rate in vacuo. Recrystallization of the resulting residue from cold (−35 °C) ether yielded large dark red-purple cubes of $MoCp^*Me_3(DIPP)$ (6.0 g, 80%): EPR ⟨g⟩ = 1.997, $\Delta\nu_{1/2}$ = 11 G, coupling to ^{97}Mo (S = 5/2) and ^{95}Mo (S = 5/2) = 38 G. Anal. Calcd for $C_{25}H_{41}OMo$: C, 66.20; H, 9.10. Found: C, 64.53, 65.44, 67.59, 65.64; H, 9.08, 8.91, 9.32, 9.05. Multiple recrystallizations of a given sample of $Cp^*MoMe_3(DIPP)$ did not improve the analytical results. The reason for this circumstance in unknown.

$MoCp^*Me_3(DOMP)$. Solid lithium 2,6-dimethoxyphenoxide (4.7 mmol, 753 mg) with vigorous stirring to a suspension of $MoCp^*Me_3(OSO_2CF_3)$ (4.7 mmol, 2.0 g) in 50 mL of cold (−35 °C) ether. A slow reaction (1 h) produced a deep red-purple solution. The reaction was filtered through Celite, and the solvent was removed from the filtrate leaving a dark red-purple semicrystalline material. This material was extracted with pentane, and the pentane was filtered through Celite. Pentane extraction was continued until the filtrate was colorless. Pentane was removed from the filtrate in vacuo, and the residue was recrystallized from the minimum volume of cold (−35 °C) ether to afford $MoCp^*Me_3(DOMP)$ as red-purple plates or cubes in two crops (1.3 g, 65%): EPR ⟨g⟩ = 1.995, $\Delta\nu_{1/2}$ = 14 G, coupling to ^{97}Mo (S = 5/2) and ^{95}Mo (S = 5/2) = 38 G. Anal. Calcd for $C_{21}H_{33}O_3Mo$: C, 58.73; H, 7.75. Found: C, 59.01; H, 7.81.

$MoCp^*Me_3(TROMP)$. Lithium 2,4,6-trimethoxyphenoxide (1.45 mmol, 276 mg) was added rapidly as a solid to a suspension of $MoCp^*Me_3(OSO_2CF_3)$ (1.41 mmol, 600 mg) in 30 mL of cold (−35 °C) ether. The reaction mixture became red-purple after 10 min. After 1 h of stirring at 25 °C, the reaction was worked up as described above for $MoCp^*Me_3(DOMP)$ to afford $MoCp^*Me_3(TROMP)$ as red-purple needles or cubes in two crops (325 mg, 50%) from ether/pentane: EPR ⟨g⟩ = 1.995, $\Delta\nu_{1/2}$ = 15 G, coupling to ^{97}Mo (S = 5/2) and ^{95}Mo (S = 5/2) = 37 G. Anal. Calcd for $C_{22}H_{35}OMo$: C, 57.51; H, 7.68. Found: C, 57.88; G, 7.82.

$MoCp^*Me_3(DMMP)$. Solid lithium 2,6-dimethyl-4-methoxyphenoxide (0.71 mmol, 112 mg) was added rapidly to a stirred suspension of $MoCp^*Me_3(OSO_2CF_3)$ (0.71 mmol, 300 mg) in 15 mL of cold (−35 °C) ether. A rapid reaction yielded a red-purple solution. After 1 h at 25 °C, the reaction was worked up as described above for $MoCp^*Me_3(DOMP)$ to afford $MoCp^*Me_3(DMMP)$ as red-purple plates or needles in two crops (200 mg, 65%): EPR ⟨g⟩ = 1.994, $\Delta\nu_{1/2}$ = 14 G, coupling to ^{97}Mo (S = 5/2) and ^{95}Mo (S = 5/2) = 37 G. Anal. Calcd for $C_{22}H_{35}O_2Mo$: C, 61.81; H, 8.25. Found: C, 61.82; H, 8.33.

$MoCp^*Me_3(OC_6F_5)$. Solid potassium pentafluorophenoxide (2.35 mmol, 522 mg) was rapidly added to a suspension of $MoCp^*Me_3(OSO_2CF_3)$ (2.35 mmol, 1 g) in 40 mL of cold (−35 °C) ether. After stirring the red solution for 1 h at 25 °C, the reaction was worked up as described above for $MoCp^*Me_3(DOMP)$ to afford $MoCp^*Me_3(OC_6F_5)$ as dark purple crystals (665 mg, 62%): EPR ⟨g⟩ = 2.000, $\Delta\nu_{1/2}$ = 14 G, coupling to ^{97}Mo (S = 5/2) and ^{95}Mo (S = 5/2) = 39 G. Anal. Calcd for $C_{19}H_{24}F_5OMo$: C, 49.68; H, 5.27. Found: C, 49.73; H, 5.30.

$MoCp^*Me_2(O_2C_6H_4)$. Solid monolithiocatecholate·(ether) (1.2 mmol, 169 mg) was rapidly added to a suspension of $MoCp^*Me_3(OSO_2CF_3)$ (1.2 mmol, 510 mg) in 15 mL of cold (−35 °C) ether. A rapid reaction yielded an orange solution containing a red-orange microcrystalline precipitate. After 1 h the reaction was worked up as described above for $MoCp^*Me_3(DOMP)$ to afford $MoCp^*Me_2(O_2C_6H_4)$ as red-orange needles (300 mg, 70%): EPR ⟨g⟩ = 2.003, $\Delta\nu_{1/2}$ = 13 G, coupling to ^{97}Mo (S = 5/2) and ^{95}Mo (S = 5/2) = 36 G, coupling to six equivalent protons (S = 1/2) = 5 G. Anal. Calcd for $C_{18}H_{25}O_2Mo$: C, 58.53; H, 6.82. Found: C, 58.54; H, 6.81.

$[MoCp^*Me_3(DIPP)][PF_6]$. $[FeCp_2][PF_6]$ (8.87 mmol, 2.935 g) was rapidly added to a stirred solution of $MoCpMe_3(DIPP)$ (9.33 mmol, 4.233 g) in 120 mL of cold (−35 °C) methylene chloride. The reaction quickly became dark red. After stirring the reaction for 2 h at 25 °C, 120 mL of pentane was added in order to precipitate a red-orange microcrystalline material. The precipitate was isolated by filtration, washed with pentane (in which it is insoluble), and dried in vacuo. This red-orange microcrystalline $[MoCp^*Me_3(DIPP)][PF_6]$ is pure enough for further use (4.5 g, 85%): ^1H NMR (CD_2Cl_2) δ 7.15–7.30 (m, 3, C_6H_3-*i*-Pr_2), 2.94 (sept, 2, $CHMe_2$), 2.03 (s, 21, $C_5(CH_3)_5$ and $Mo(CH_3)_{cis}$), 1.39 (s, 3, $Mo(CH_3)_{trans}$), 1.27 (d, 12, $CH(CH_3)_2$); ^{13}C NMR (CD_2Cl_2) δ 159.73 (s, C_{ipso}), 140.16 (s, C_{aryl}), 128.18 (d, C_{aryl}), 125.00 (d, C_{aryl}), 118.72 (s, $C_5(CH_3)_5$), 59.03 (q, $Mo(CH_3)_{cis}$), 48.90 (q, $Mo(CH_3)_{trans}$), 27.53 (d, $CHMe_2$), 24.32 (q, $CH(CH_3)_2$), 11.36 (q, $C_5(CH_3)_5$). Anal. Calcd for $C_{25}H_{41}OMoPF_6$: C, 50.17; H, 6.91. Found: C, 49.77, H, 6.84.

$[MoCp^*Me_3(DOMP)][PF_6]$. $[FeCp][PF_6]$ (1.15 mmol, 381 mg) was rapidly added to a stirred solution of $MoCp^*Me_3(DOMP)$ (1.18 mmol, 505 mg) in 10 mL of cold (−35 °C) methylene chloride. The reaction quickly became dark red. After 1 h at 25 °C, 30 mL of pentane was added to the reaction mixture in order to precipitate a dark brown microcrystalline solid. This precipitate was isolated by filtration, washed with pentane and ether, and dried in vacuo. This dark brown microcrystalline $[MoCp^*Me_3(DOMP)][PF_6]$ is pure enough for further use (580 mg, 88%): ^1H NMR (CD_2Cl_2) δ 7.21 (t, 1, H_{para}), 6.61 (d, 2, H_{meta}), 3.90 (s, 6, OCH_3), 2.02 (s, 15, $C_5(CH_3)_5$), 1.96 (s, 6, $Mo(CH_3)_{cis}$), 1.58 (s, 3, $Mo(CH_3)_{trans}$); ^{13}C NMR (CD_2Cl_2) δ 159.29 (s, C_{ipso}), 151.71 (s, C_{aryl}), 129.19 (d, C_{aryl}), 118.47 (s, $C_5(CH_3)_5$), 105.02 (d, C_{aryl}), 59.74 (q, OCH_3 or $Mo(CH_3)$), 56.94 (q, OCH_3 or $Mo(CH_3)$), 56.36 (q, OCH_3 or $Mo(CH_3)$), 11.65 (q, $C_5(CH_3)_5$). Anal. Calcd for $C_{21}H_{33}O_3MoPF_6$: C, 43.91; H, 5.79. Found: C, 43.99; H, 5.79.

$[MoCp^*Me_3(TROMP)][PF_6]$. $[FeCp_2][PF_6]$ (0.57 mmol, 189 mg) was rapidly added to a stirred solution of $MoCpMe_3(TROMP)$ (0.58 mmol, 268 mg) in 5 mL of cold (−35 °C) methylene chloride. The reaction immediately became deep purple. After 1 h at 25 °C 15 mL of pentane was added to the reaction mixture in order to precipitate a dark brown-purple microcrystalline solid. This precipitate was isolated by filtration, washed with pentane and ether, and dried in vacuo. This dark brown-purple microcrystalline $[MoCp^*Me_3(TROMP)][PF_6]$ is pure enough for further use (300 mg, 87%): ^1H NMR (CD_2Cl_2) δ 6.15 (s, H_m), 3.89 (s, 6, ortho OCH_3), 3.87 (s, 3, para OCH_3), 1.99 (s, 15, $C_5(CH_3)_5$), 1.78 (s, 6, $Mo(CH_3)_{cis}$), 1.59 (s, 3, $Mo(CH_3)_{trans}$); ^{13}C NMR (CD_2Cl_2) δ 162.00 (s, C_{aryl}), 153.17 (s, C_{aryl}), 140.93 (s, C_{aryl}), 117.74 (s, $C_5(CH_3)_5$), 91.66 (d, C_{meta}), 58.46 (overlapping q, OCH_3 or $Mo(CH_3)$), 56.49 (overlapping q, OCH_3 or $Mo(CH_3)$), 11.69 (q, $C_5(CH_3)_5$). Anal. Calcd for $C_{22}H_{35}O_4MoPF_6$: C, 43.72; H, 5.84. Found: C, 43.78, H, 5.86.

$[MoCp^*Me_3(DMMP)][PF_6]$. $[FeCp_2][PF_6]$ (0.43 mmol, 141 mg) was rapidly added to a stirred solution of $MoCp^*Me_3(DMMP)$ (0.44 mmol, 186 mg) in 5 mL of cold (−35 °C) methylene chloride. The reaction immediately became red-purple. After 1 h at 25 °C 15 mL of pentane was added to the reaction mixture in order to precipitate a red-brown microcrystalline solid. The precipitate was isolated by filtration, washed with pentane and ether, and dried in vacuo to afford $[MoCp^*Me_3(DMMP)][PF_6]$ as a red-brown solid that was pure enough for further use (200 mg, 81%): ^1H NMR (CD_2Cl_2) δ 6.58 (s, 2, H_m), 3.78 (s, 3, OCH_3), 2.30 (s, 6, CH_3), 2.01 (s, 15, $C_5(CH_3)_5$), 1.94 (s, 6, $Mo(CH_3)_{cis}$), 1.38 (s, 3, $Mo(CH_3)_{trans}$); ^{13}C NMR (CD_2Cl_2) δ 159.01 (s, C_{ipso}), 158.48 (s, C_{aryl}), 132.45 (s, C_{aryl}), 118.20 (s, $C_5(CH_3)_5$), 114.51 (d, C_{meta}), 57.10 (q, OCH_3 or $Mo(CH_3)$), 55.97 (q, OCH_3 or $Mo(CH_3)$), 49.27 (q, OCH_3 or $Mo(CH_3)$), 18.62 (q, $-CH_3$), 11.69 (q, $C_5(CH_3)_5$). Anal. Calcd for $C_{22}H_{35}O_2MoPF_6$: C, 46.16; H, 6.16. Found: C, 45.95; H, 6.15.

$[MoCp^*Me_3]_2(\mu\text{-}N_2)$. (a) Neat hydrazine (5.0 mmol, 159 μL) was rapidly added to a vigorously stirred suspension of $[MoCp^*Me_3(DIPP)][PF_6]$ (1.67 mmol, 1.0 g) in 60 mL of cold (−35 °C) ether. $[MoCp^*Me_3(DIPP)][PF_6]$ reacts over a period of 10 min to yield a red solution that contains a tan precipitate. The reaction mixture was filtered through Celite, and the solvent was removed from the filtrate to yield a red-brown oil. This oil was extracted with the minimum volume of pentane, and the resulting red solution was passed through a plug of deactivated alumina (7% H_2O, 1 cm length × 3 cm width) in order to remove excess phenol, $MoCp^*Me_3(DIPP)$, and other polar side products.

The pentane was then removed from the filtrate in vacuo, and the resulting dark residue was recrystallized from the minimum volume of cold (−35 °C) ether to afford $[Cp^*MoMe_3]_2(\mu\text{-}N_2)$ as black plates or cubes in three crops (80 mg, 16%): ^1H NMR (C_6D_6) δ 1.55 (s, 15, $C_5(CH_3)_5$), 1.08 (s, 6, $Mo(CH_3)_{cis}$), 0.81 (s, 3, $Mo(CH_3)_{trans}$); ^1H NMR (CD_2Cl_2) δ 1.58 (s, 15, $C_5(CH_3)_5$), 0.60 (s, 6, $Mo(CH_3)_{cis}$), 0.09 (s, 3, $Mo(CH_3)_{trans}$); IR (thin film on KBr, cm^{-1}) 2877–2973 (s, ν_{CH}), 1426–1485 (s, ν_{CH}), 1381 s, 1166 m, 1146 w, 1135 w, 1123 w, 1073 w, 1025 s, 932 s, 823 s, 803 w, 741 w, 720 w, 663 w, 483 s. Anal. Calcd for $C_{26}H_{48}N_2Mo_2$: C, 53.79; H, 8.33; N, 4.82. Found: C, 53.97; H, 8.29; N, 4.97.

(b) Neat hydrazine (1.58 mmol, 50 μL) was rapidly added to a vigorously stirred suspension of $[MoCp^*Me_3(DOMP)][PF_6]$ (0.52 mmol, 300 mg) in 5–10 mL of cold (−35 °C) petane or ether. $[MoCp^*Me_3(DOMP)][PF_6]$ reacts quickly to yield a colorless solution, which then further reacts slowly over 1 h to yield a red solution that contains a brown/tan precipitate. The reaction mixture was filtered through Celite, and the solvent was removed from the filtrate yielding a dark red-brown oil. Proton NMR indicates that the filtrate is composed of $[MoCp^*Me_3]_2(\mu\text{-}N_2)$ contaminated with varying amounts of $MoCp^*Me_3(O)$[8], HDOMP, and other diamagnetic products. *No $MoCp^*Me_3(DOMP)$ is produced in this reaction.* Most of the impurities (except HDOMP) cannot be removed by column chromatography, and $[MoCp^*Me_3]_2(\mu\text{-}N_2)$ cannot be isolated by recrystallization. Similar results are obtained starting with $[MoCp^*Me_3(DMMP)][PF_6]$ or $[MoCp^*Me_3(TROMP)][PF_6]$ and proceeding as described above.

$[MoCp^*Me_3](\mu\text{-}N_2)[WCp'Me_3]$. $[MoCp^*Me_3(DOMP)][PF_6]$ (1.37 mmol, 785 mg) was added rapidly to a vigorously stirred solution of $WCp'Me_3(NNH_2)$ (1.37 mmol, 560 mg) and NEt_3 (1.43 mmol, 200 μL) in 40 mL of cold ether (−35 °C). $[MoCp^*Me_3(DOMP)][PF_6]$ reacts slowly over 2 h to yield a red solution and a tan precipitate. The reaction mixture was filtered through Celite, and the solvent was removed from the filtrate leaving behind a red-brown oily residue. This residue was extracted with pentane, the pentane was filtered through Celite, and the solvent was removed from the filtrate in vacuo. Recrystallization of this residue from pentane or ether/pentane (~3/1 ratio of volumes) yielded $[MoCp^*Me_3]\mu\text{-}N_2[WCp'Me_3]$ as dark red cubes (500 mg, 53%) contaminated with 10–20% of $[WCp'Me_3]_2(\mu\text{-}N_2)$. Recrystallization from ether/pentane at least 3 times decreases the contamination to 3–15%. $[MoCp^*Me_3](\mu\text{-}N_2)[WCp'Me_3]$ also can be prepared from $[MoCp^*Me_3(DMMP)][PF_6]$ or $[MoCp^*Me_3(TROMP)][PF_6]$ in an analogous manner to that described for $[MoCp^*Me_3(DOMP)][PF_6]$ above, although if $[MoCp^*Me_3(DIPP)][PF_6]$ is used the yield of $[MoCp^*Me_3](\mu\text{-}N_2)[WCp'Me_3]$ is somewhat lower (20%), and contamination of the product with $[WCp'Me_3]_2(\mu\text{-}N_2)$ is significantly higher (30–40%): ^1H NMR (C_6D_6) δ 2.08 (q, 2, $C_5(CH_3)_4(CH_2CH_3)$), 1.68 (s, 6, $C_5(CH_3)_4(CH_2CH_3)$), 1.60 (s, 15, $C_5(CH_3)_5$), 1.58 (s, 6, $C_5(CH_3)_4(CH_2CH_3)$), 1.08 (s, 6, $M(CH_3)_{cis}$), 1.05 (s, 6, $M(CH_3)_{cis}$), 0.78 (t, 3, $C_5(CH_3)_4(CH_2CH_3)$), 0.76 (s, 3, $M(CH_3)_{trans}$), 0.71 (s, 3, $M(CH_3)_{trans}$); ^1H NMR (CD_2Cl_2) δ 2.20 (q, 2, $C_5(CH_3)_4(CH_2CH_3)$), 1.89 (s, 6, $C_5(CH_3)_4(CH_2CH_3)$), 1.84 (s, 6, $C_5(CH_3)_4(CH_2CH_3)$), 1.75 (s, 15, $C_5(CH_3)_5$), 1.03 (t, 3, $C_5(CH_3)_4(CH_2CH_3)$), 0.61 (s, 6, $M(CH_3)_{cis}$), 0.51 (s, 6, $M(CH_3)_{cis}$), 0.21 (s, 3, $M(CH_3)_{trans}$), 0.05 (s, 3, $M(CH_3)_{trans}$); $^{13}C\{^1H\}$ NMR (CD_2Cl_2) δ 114.8, 111.16, 110.08, 109.39 (Cp ring carbons), 36.77, 38.83 ($M(CH_3)_{trans}$), 29.15, 29.14 ($M(CH_3)_{cis}$), 19.90 ($Cp'CH_2CH_3$), 14.48 ($Cp'CH_2CH_3$), 10.88–11.05 (overlapping, Cp methyl carbons); IR (thin film on KBr, cm^{-1}) 2935–2963 (s, ν_{CH}), 1429–1486 (s, ν_{CH}), 1384 s, 1378 s, 1168 m, 1070 w, 1052 w, 1026 s, 862 m, 841 s, 484 s. Anal. Calcd for $C_{27}H_{50}N_2MoW$: C, 47.51; H, 7.38; N, 4.10. Found: C, 47.32; H, 7.37; N, 4.36.

Protonation Studies. The dinitrogen complexes (3–4 × 10^{-2} mmol) were dissolved in 2–4 mL of cold (−35 °C) solvent (THF or ether) under dinitrogen, and 16 equiv of lutidine·HX (X = Cl, OSO_2CF_3) and 12 equiv of amalgamated zinc[22] (or 0.5% Na/Hg in one case) were added simultaneously and with vigorous stirring. The reaction flask was then sealed with a rubber septum, and the stirring continued. The reaction mixtures slowly changed color (usually to a dark red/brown). After 24 h at 25 °C, 100 μL of concentrated HCl was added to the reaction mixture by syringe. The solvent was then immediately removed in vacuo, and the residue was treated with 15 mL of a 4.0 M NaOH solution in a closed system under argon. The basic solution was then gently distilled under argon into 15 mL of 0.5 N H_2SO_4 until ~10–15 mL had been collected. The volume of the acid solution was then brought up to 30 mL with distilled water. This solution was tested quantitatively for ammonia and hydrazine by using the indophenol[21] and *p*-(dimethylamino)benzaldehyde[22] tests, respectively. An identical procedure was used to quantify the amount of ammonia and hydrazine produced from all three of the nitrogen complexes. In the cases when no electron source was employed 25 equiv of concentrated HCl was present instead of lutidine·HX.

In one case (W/Mo; Lut·HCl; THF; Zn/Hg; see Table VI) the base distillation step was omitted. The residue was simply extracted with water and filtered and analyzed in the normal manner. Essentially the same result was obtained.

X-ray Study of $[MoCp^*Me_3]_2(\mu\text{-}N_2)$. A black rod-like crystal of $[MoCp^*Me_3]_2(\mu\text{-}N_2)$ having approximate dimensions 0.800 × 0.420 × 0.420 mm was mounted on a glass fiber. Data were collected at −65 °C on an Enraf-Nonius CAD-4 diffractometer with graphite monochromated Mo Kα radiation. A total of 6865 reflections ($+h,+k,\pm l$) were collected in the range $3° < 2\theta < 55°$ with 5489 having $I_0 > 3\sigma(I_0)$ being used in the structure refinement which was by full-matrix least-squares techniques (271 variables) with use of the TEXSAN crystallographic software package from Molecular Structure Corporation. Final $R = 0.032$ and $R_w = 0.043$. The non-hydrogen atoms were refined anisotropically. Hydrogen atoms were included in the structure factor calculation in idealized positions ($d_{C\text{-}H} = 0.95$ Å). An empirical absorption correction was applied. Solution and refinement proceeded without difficulty. The maximum and minimum peaks on the final difference Fourier map corresponded to 0.52 and −0.70 $e^-/Å^3$, respectively. Crystal data are as follows: $a = 12.895$ (5) Å, $b = 16.443$ (6) Å, $c = 14.556$ (5) Å, $\beta = 115.87$ (3)°, $V = 2777$ (4) $Å^3$, space group = $P2_1/n$ (no. 14), $Z = 4$, mol wt = 580.56, ρ(calcd) = 1.388 g/cm^3, μ = 8.96 cm^{-1}.

X-ray Study of $[MoCp^*Me_3](\mu\text{-}N_2)[WCp'Me_3]$. A black prism of $[MoCp^*Me_3](\mu\text{-}N_2)[WCp'Me_3]$ having approximate dimensions 0.350 × 0.350 × 0.350 mm was mounted on a glass fiber. Data were collected at −65 °C on a Rigaku AFC6R diffractometer with graphite monochromated Mo Kα radiation and a 12 KW rotating anode generator. A total of 7082 reflections ($+h,+k,\pm l$) were collected in the range $4° < 2\theta < 55°$ with 4810 having $I_0 > 3\sigma(I_0)$ being used in the structure refinement which was by full-matrix least-squares techniques (289 variables) with use of the TEXSAN crystallographic software package from Molecular Structure Corporation. Final $R = 0.031$ and $R_w = 0.045$. The non-hydrogen atoms were refined anisotropically. Hydrogen atoms were included in the structure factor calculation in idealized positions ($d_{C\text{-}H} = 0.95$ Å). An empirical absorption correction was applied. The crystal contained 12% $[WCp'Me_3]_2(\mu\text{-}N_2)$ dopant, a conclusion arrived at by systematically varying the occupancy until the thermal parameters of both the tungsten (from $[MoCp^*Me_3](\mu\text{-}N_2)[Cp'WMe_3]$) and the tungsten (from the dopant) were equivalent. The maximum and minimum peaks on the final difference Fourier map corresponded to 0.84 and −0.67 $e^-/Å^3$, respectively. Crystal data are as follows: $a = 13.46$ (2) Å, $b = 16.46$ (2) Å, $c = 14.48$ (2) Å, $\beta = 116.92$ (9)°, $V = 2861$ (6) $Å^3$, space group = $P2_1/n$ (no. 14), $Z = 4$, mol wt = 693.04, ρ(calcd) = 1.609 g/cm^3, μ = 49.88 cm^{-1}.

Acknowledgment. R.R.S. thanks the National Institutes of Health for support through Grant GM 31978. We also thank the U.S. Department of Energy, Division of University and Industry Programs, for funds to purchase the X-ray diffractometer (Grant DE-FG05-86ER 75292) and D. Coucouvanis for helpful discussions. M.G.V. thanks the National Science Foundation for a predoctoral fellowship.

Registry No. $MoCp^*Me_4$, 126112-52-5; $MoCp^*Cl_4$, 96055-87-7; $MoCp^*Me_3(OSO_2CF_3)$, 126112-53-6; $MoCp^*Me_3(DIPP)$, 126112-55-8; $MoCp^*Me_3(DOMP)$, 126112-56-9; $MoCp^*Me(TROMP)$, 126112-57-0; $MoCp^*Me_3(DMMP)$, 126133-00-4; $MoCp^*Me_3(DC_6F_5)$, 126112-58-1; $MoCp^*Me_2(O_2C_6H_4)$, 126112-59-2; $[MoCp^*Me_3(DIPP)][PF_6]$, 126112-61-6; $[MoCp^*Me_3(DOMP)][PF_6]$, 126112-63-8; $[MoCp^*Me_3(TROMP)][PF_6]$, 126112-65-0; $[MoCp^*Me(DMMP)][PF_6]$, 126112-67-2; $[MoCp^*Me_3]_2(\mu\text{-}N_2)$, 126112-68-3; $[MoCp^*Me_3]\mu\text{-}N_2[WCp'Me_3]$, 126112-71-8; $WCp'Me_3(NNH_2)$, 126112-69-4; $[WCp'Me_3]_2(\mu\text{-}N_2)$, 126112-70-7; $[FeCp_2][PF_6]$, 11077-24-0; Li(DIPP)·(ether), 98193-96-5; Li(DOMP), 98171-22-3; Li(TROMP), 126112-50-3; Li(DMMP), 126112-51-4; $K(OC_6F_5)$, 4615-85-4; monolithiocatecholate·(ether), 126112-54-7; hydrazine, 302-01-2; lutidine·HCl, 15439-85-7; lutidine·$HOSO_2CF_3$, 119503-59-2; ammonia, 7664-41-7.

Supplementary Material Available: Tables of final positional and anisotropic thermal parameters, temperature factors, bond distances for non-hydrogen atoms, and bond angles for non-hydrogen atoms for $[MoCp^*Me_3](\mu\text{-}N_2)[WCp'Me_3]$ and $[MoCp^*Me_3]_2(\mu\text{-}N_2)$ (18 pages); tables of observed and calculated structure factors (76 pages). Ordering information is given on any current masthead page.

(22) (a) Caesar, P. D. *Organic Synthesis*; Wiley: New York, 1963; Collect. Vol. 4, p 695. (b) Fieser, L. F.; Fieser, M. *Reagents for Organic Synthesis*; Wiley: New York, 1967; p 1287.